JOURNAL OF AGRICULTURAL AND FOOD CHEMISTRY

pubs.acs.org/JAFC

Article

Genome Mining Reveals Biosynthesis of the Antifungal Lipopeptaibols, Texenomycins, through a Hybrid PKS-NRPS System, in the Fungus *Mariannaea elegans*

Yang Jiao,[⊥] Jian Ling,[⊥] Raja Asad Ali Khan, Ning Luo, Zixin Li, Zeyu Li, Yuhong Yang, Jianlong Zhao, Zhenchuan Mao, Gerald F. Bills,* Bingyan Xie,* and Yan Li*

Cite This: *J. Agric. Food Chem.* 2025, 73, 226−236

Read Online

ACCESS | Metrics & More | Article Recommendations | Supporting Information

ABSTRACT: Texenomycins are a family of linear lipopeptaibols with a long polyketide side chain at the N-terminus and 21 amino acid residues at the C-terminus, presenting demonstrated potential as antibiotics against plant fungal pathogens. In this study, texenomycins were identified and isolated from the fungus *Mariannaea elegans* strain TTI-0396 and showed effective antifungal properties against two plant pathogens *Colletotrichum lagenarium* and *Botrytis cinerea*. Through analysis of the whole-genome data of *M. elegans* strain TTI-0396, we discovered a hybrid PKS-NRPS system with the polyketide synthase (PKS: TexQ), thioesterase (TexO), acyl-CoA ligase (TexI), and three nonribosomal peptide synthetases (NRPSs: TexG, TexJ, TexV) in the *tex* gene cluster that were proposed to be responsible for the biosynthesis of texenomycins and another related lipopeptaibol, lipohexin. The functions of six key genes (*texQ*, *texO*, *texI*, *texG*, *texJ*, and *texV*) in the hybrid PKS-NRPS system were verified by gene deletion experiments, and five genes (*texQ*, *texO*, *texI*, *texG*, and *texV*) were confirmed to be responsible for the biosynthesis of texenomycins, while four genes (*texQ*, *texO*, *texI*, and *texJ*) were involved in the biosynthesis of lipohexin. Furthermore, the function of one transcription factor gene (*texR*), which enhanced the production of texenomycins by regulating the key genes in the *tex* gene cluster, was also demonstrated through gene deletion and overexpression experiments. Finally, a hypothetical scheme for texenomycins and lipohexin biosynthesis assembly is proposed. The elucidation of this intricate hybrid PKS-NRPS system has significantly deepened our comprehension of the mechanisms underlying the generation and chemical diversity of fungal lipopeptaibol natural products, offering a promising avenue for future research and potential applications in fungicidal disease control in agriculture.

KEYWORDS: *Mariannaea elegans, antifungal lipopeptaibols, genome mining, biosynthetic genes, hybrid PKS-NRPS system*

INTRODUCTION

Fungal plant diseases can cause huge losses to the growth and yield of crops, leading to significant economic losses.[1] *Colletotrichum lagenarium* and *Botrytis cinerea* are the most common plant pathogenic fungi distributed worldwide. They infect over 1400 plant species causing severe pre- and postharvest gray mold decay on many important economic crops and horticultural crops.[2] Fungicides and breeding-resistant cultivars are the primary methods of controlling fungal diseases. However, traditional disease-resistant breeding approaches struggle to meet the demands of agriculture due to a long breeding cycle and rapid pathogen variation. Additionally, fungicide-resistant pathogens have also become a widespread and severe problem, threatening crop quality and yield security. Recently, utilizing effective biocontrol microorganisms and developing their antifungal agents (microbial natural products) to control fungal plant diseases has become increasingly popular.

Mariannaea elegans (Ascomycota, Hypocreales, Nectriaceae, Figure S1) was reported as a pathogen of some insects and reptiles and belongs to the Nectriaceae, a family of fungi that includes important plant pathogens, such as *Fusarium*, as well as species that are used extensively in industrial and commercial applications, including as the biocontrol agents and the sources of gibberellic acid, zearalenone, and lipopeptaibols.[3] Lipopeptaibols are a special class of naturally occurring 6−21 peptides with antimicrobial activity, characterized by an 8−15 carbon fatty chain at the N-terminus and a high content of α,α-dialkylated nonproteinogenic amino acids at the C-terminus, and as a new generation of agricultural chemical alternatives, they have been increasingly studied in recent years.[4] They are primarily derived from fungi, especially *Trichoderma* spp., and have been shown to possess biological activity against plant pathogenic bacteria, fungi, and oomycetes.[5−9] Their mechanisms of action are primarily mediated through direct interaction with biological membranes or by the inhibition or disruption of metabolic pathways.[9−11] Texenomycins and lipohexin are lipopeptaibols that were initially found in the fungus *Moeszia lindtneri* (later identified as *M. elegans*) and could form channels in bilayer membranes, resulting in cell leakage and loss of anions.[12,13] Structurally, texenomycins consist of one 2-methyl-3-oxo-tetradecanoyl (MOTDA) residue at the N-

Received: September 19, 2024
Revised: December 9, 2024
Accepted: December 10, 2024
Published: December 20, 2024

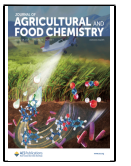

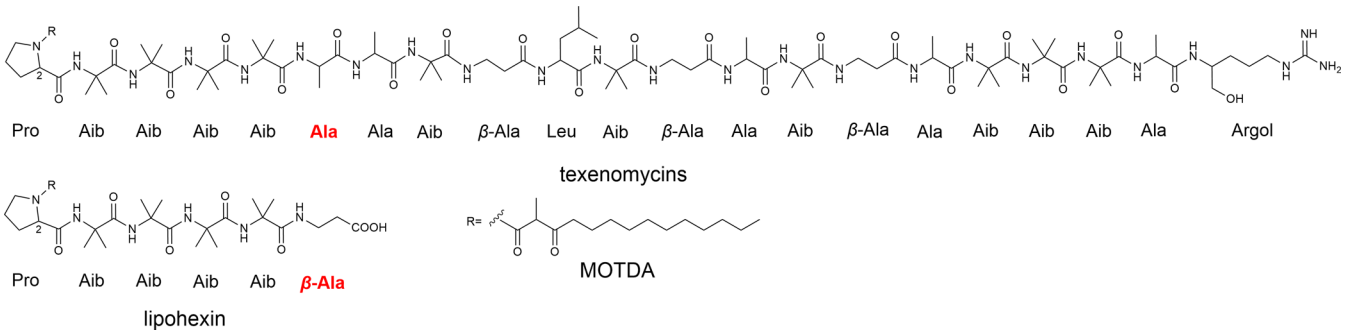

Figure 1. Structure of texenomycins and lipohexin.

terminal and 21 amino acid residues at the C-terminal, while lipohexin possesses MOTDA residue at the N-terminal and the same first five amino acid residues (except for the sixth β-Ala in lipohexin) as those in texenomycins at the C-terminal (Figure 1). To our knowledge, there is no existing research on the biosynthetic pathways related to these two lipopeptaibols, texenomycins, and lipohexin.

In this study, the 21-mer and 6-mer lipopeptaibols, texenomycins, and lipohexin were codiscovered in the fungus *M. elegans* strain TTI-0396, and texenomycins showed strong biological activities against two plant pathogens, *C. lagenarium* and *B. cinerea*. The discovery of this phenomenon enriches the functions of texenomycins and provides new avenues for the diverse applications of agricultural antibiotics and the development of antiresistance drugs. Furthermore, the whole genome of *M. elegans* strain TTI-0396 was sequenced, assembled, and annotated. Genome analysis revealed that a complex hybrid PKS-NRPS system was involved in the texenomycins' biosynthetic gene cluster (*tex*), which encodes the biosynthesis of both texenomycins and lipohexin. In addition, the functions of seven key genes in the *tex* cluster were demonstrated by gene knockout experiments and liquid chromatography-mass spectrometry (LC-MS) analysis of the mutants. Finally, a hypothetical biosynthetic pathway for both texenomycins and lipohexin was proposed. The occurrence of a single gene cluster synthesizing lipopeptaibols of two different lengths is rarely reported in fungi, which aids in deepening our understanding of how organisms synthesize complex molecules. The antifungal activities of texenomycins against pathogenic fungi may provide a potential application in agriculture.

EXPERIMENTAL PROCEDURES

Strains. *M. elegans* strain TTI-0396 isolated from cow manure collected along Sawmill Rd., Brazoria County, Texas, was maintained on potato dextrose agar (PDA). *B. cinerea* and *C. lagenarium* were isolated from cucumber and deposited in the Agricultural Culture Collection of China (ACCC39683) and China General Microbiological Culture Collection Center (CGMCC 3.2198), respectively. *Escherichia coli* Trelief 5α chemically competent cells used for molecular cloning, were purchased from Beijing Tsingke Biotech Co., Ltd.

Media and Culture Conditions. Potato dextrose broth (PDB) and PDA for fungal cultures were purchased from Difco (BD). Seed cultures for growing *M. elegans* were used in SMYA medium (40 g of maltose, 10 g of yeast extract, 10 g of peptone, 4 g of agar per liter of deionized H_2O) at 28 °C and 220 rpm for 5 days. *M. elegans* strain TTI-0396 were grown on wheat solid medium (30 g of wheat seeds and 50 mL of base liquid containing 2 g of yeast extract, 10 g of sodium tartrate, 1 g of K_2HPO_4, 1 g of $MgSO_4{\cdot}7H_2O$, 0.05 g $FeSO_4{\cdot}7H_2O$ per liter of deionized H_2O) in static culture at 28 °C for 14 days, and MOF liquid medium (75 g of mannitol, 15 g of oat flour, 5 g of yeast extract, 4 g of L-glutamic acid, 16.2 g of MES per liter of deionized H_2O) at 28 °C for 14 days at 220 rpm. T-Top medium (0.5 g of KCl, 0.5 g of $MgSO_4{\cdot}7H_2O$, 1.0 g of KH_2PO_4, 2 g of $NaNO_3$, 200 g of sucrose, 20 g of glucose, and 10 g of agar per liter of deionized H_2O) was used for protoplast regeneration.

Extraction and Isolation. Texenomycins were separated by an antifungal-guided fractionation protocol.[14] A total of ten 500 mL flasks of wheat fermented culture were extracted twice with 1.0 L ethyl acetate (100 mL for each 500 mL fermentation flask), and the organic phase was evaporated to dryness under vacuum using a rotavapor apparatus (N-1300, EYELA, Tokyo, Japan) to obtain the crude extract (3.2 g). The crude extract was preseparated with a Sephadex LH-20 column using MeOH/chloroform ($CHCl_2$) (1:1) as the mobile phase, and the active fractions (780 mg) inhibiting growth of those test fungal pathogens were combined. Further purification was carried out by an Agilent 1260 HPLC system with a semipreparative reverse phase HPLC column (Agilent Zorbax SB C18; 5 μm; 9.4 mm × 250 mm) using the conditions: gradient elution 90−100% acetonitrile in water over 15 min; 2 mL/min, to afford texenomycins (58.8 mg, t_R 8.5 min).

LC-MS Analysis. The concentrated extract was dissolved in methanol and used for liquid chromatography/mass spectrometry (LC-MS) analysis. Samples were analyzed using an Agilent 1260 HPLC system coupled with Agilent G6530B High-Definition Accurate-Mass Quadrupole Time-of-Flight (Q-TOF) equipped with an electrospray ionization (ESI) source operated in positive ion mode. Ten μL of each dissolved extract was injected for LC-MS analysis. A linear gradient of 10−100% acetonitrile in water (with 0.1% formic acid) for 20 min at a flow rate of 1.0 mL/min through an Agilent Zorbax SB-C18 reversed-phase column (4.6 mm × 150 mm, 5 μm) was used. For Q-TOF/MS conditions, the fragmentor and capillary voltages were kept at 65 and 1800 V, respectively. Nitrogen was provided as the nebulizing and drying gas (300 °C) with a flow rate of 10.0 L/min, and the pressure of the nebulizer was 35 psi. The MS scan range was 500−2500 *m*/*z*, and MS-MS scan range was 40−1500 *m*/*z*.

Antifungal Minimum Inhibitory Concentration (MIC) Assay. The antifungal MIC assay was performed by the broth microdilution method according to the National Committee for Clinical Laboratory Standards (NCCLS, 2000) using the serial dilution method in 96-well plates containing PDB as the growth medium. The test compound was dissolved in DMSO and serially diluted in the growth medium. Growth was assessed at 24 h by adding 10% PrestoBlue resazurin dye (Thermo Fisher Scientific) and incubating in the dark at 37 °C until color developed. Visual end point and optical density readings of the microplate wells were measured relative to the test compound, and the positive control (hygromycin B) and negative control (pure growth medium). The MIC value was defined as the lowest concentration of a test compound that resulted in a culture with a density consistent with 100% inhibition and no detectable growth as observed by microscopy when compared to the growth of the untreated control. Each of the fungal pathogens was tested in triplicate.

Genome Sequencing, Assembly, and Annotation. *M. elegans* strain TTI-0396 genome was sequenced by Nextomics Biosciences (Wuhan, China) using the PacBio Sequael and Illumina NovaSeq platforms. The genome was assembled using Canu version 1.6 (https://github.com/marbl/canu/releases) and polished based on pacBio reads

https://doi.org/10.1021/acs.jafc.4c08847
J. Agric. Food Chem. 2025, 73, 226−236

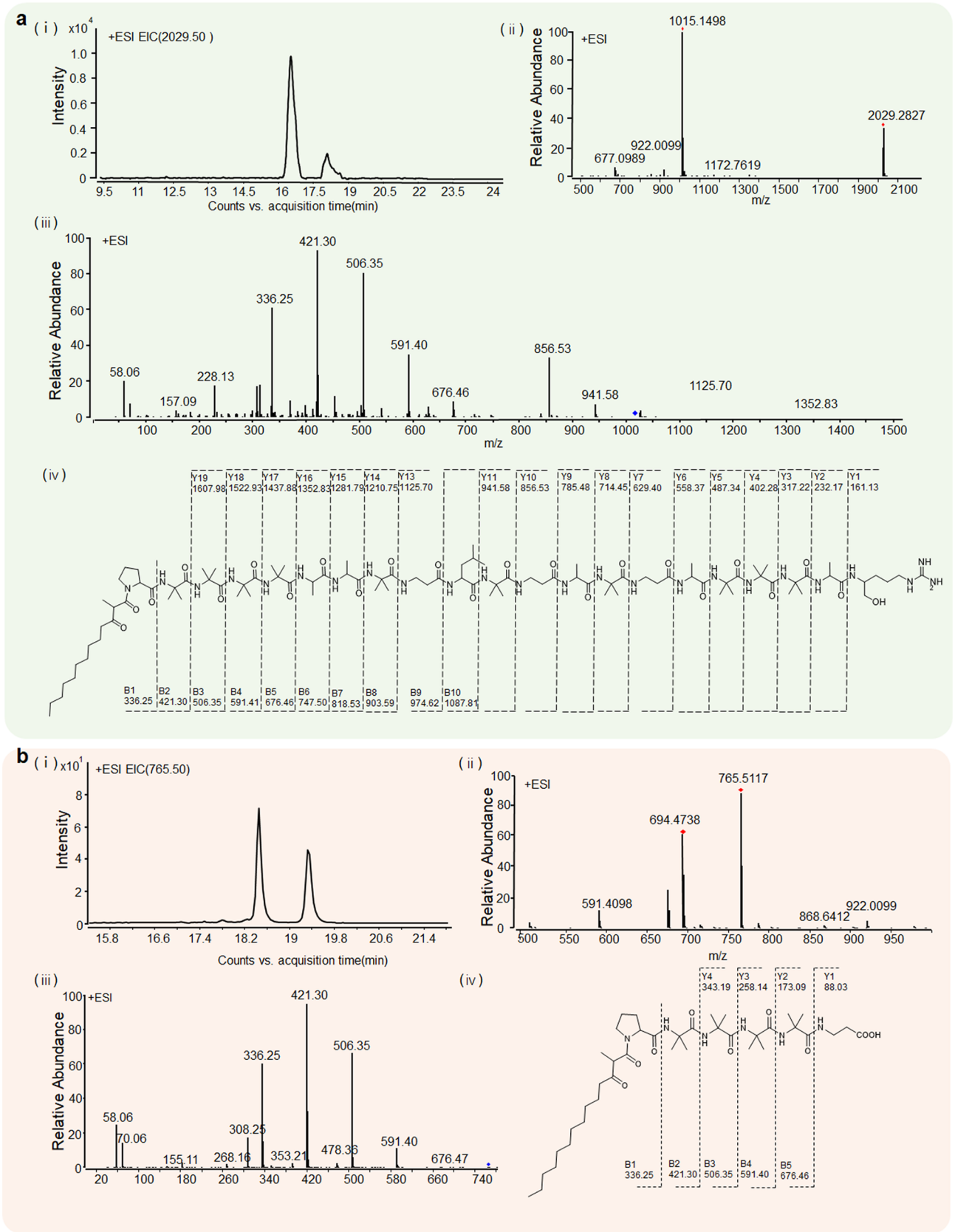

Figure 2. Chemical analysis of texenomycins and lipohexin. (a) Chemical analysis of texenomycins. LC-MS analysis of texenomycins (i). HRESI-MS spectrum of texenomycins (ii). ESI-MS-MS spectrum of texenomycins (iii). ESI-MS-MS fragmentation irons patterns for texenomycins (iv). (b) Chemical analysis of lipohexin. LC-MS analysis of lipohexin (i). HRESI-MS spectrum of lipohexin (ii). ESI-MS-MS spectrum of lipohexin (iii). ESI-MS-MS fragmentation irons patterns for lipohexin (iv).

https://doi.org/10.1021/acs.jafc.4c08847
J. Agric. Food Chem. 2025, 73, 226−236

using racon version 1.4.3 (https://github.com/isovic/racon) with the default parameters.[15] The repetitive sequences were annotated by combining ab initio and homology-based methods using Repbase (http://www.girinst.org/repbase). *De novo* gene structure annotation was predicted using four different suites of softwares: Augustus (V 3.3.2, http://augustus.gobics.de/), GeneMaker (V2.6 https://softgenetics.com/products/genemarker/), GlimmerHMM V3.0.4, and SNAP (https://github.com/KorfLab/SNAP).[16−20] Functional annotation was carried out using the UniProt (https://ftp.uniprot.org/pub/databases/uniprot/), Pfam (http://pfam-legacy.xfam.org/), KEGG (https://www.genome.jp/kegg/), GO (https://www.geneontology.org/), COG (KOG), and CAZyme databases (http://www.cazy.org/).[21−25] Potential secreted proteins were predicted by SignalP 3.0.[26] A circular genome of *M. elegans* was visualized using Circos version 0.8.2 (http://circos.ca/software).[27]

Phylogenetic Relationship Analysis. Multiprotein species trees were built from single-copy genes from *M. elegans* strain TTI-0396 and 20 other fungi. The single-copy genes were identified by an OrthoFinder (version 0.7.1), and genomic information involved in the analysis is shown in Table S1.[28] The alignment of concatenated sequences was performed using MAFFT.[29] A maximum likelihood tree was constructed for concatenated alignments with IQ-TREE using 1000 replicates as bootstraps and the best substitution model proposed by the same tool.[30]

Quantitative Real-Time PCR Analysis. After 14 days of fermentation on PDB and MOF, the mycelium was collected by filtration for quantitative real-time PCR (qRT-PCR) analysis, and Total RNA was extracted using an RNA Isolater Total RNA Extraction Reagent (Vazyme, Nanjing, China). First-strand complementary DNA (cDNA) was synthesized using the PrimeScript RT reagent Kit with gDNA Eraser (TaKaRa, Japan). The qRT−PCR reactions were performed in three technical replicates and three biological replicates in each reaction. qPCR was performed using TB Green Premix Ex *Taq*II (TaKaRa, Japan) on a Bio-Rad CFX96 instrument (Bio-Rad). The β-tubulin gene (HMA_4) was chosen as the reference to normalize gene expression measurements. The relative expression was calculated using the $2^{-\Delta\Delta Ct}$ method.[31] The primers used for qRT−PCR analysis listed in Table S2.

Molecular Biological Manipulations. The genomic DNA of *M. elegans* strain TTI-0396 and its transformants were prepared by Plant Direct PCR Kit (Herogen Bio). The high-fidelity DNA polymerase Phanta Flash Master Mix (Vazyme, China) was used to amplify DNA fragments. For diagnostic PCR, Taq Polymerase from Taq Master Mix (Vazyme, China) was used. The vectors were constructed by an efficient homologous-recombinant-based method following the protocol of ClonExpress MultiS One Step Cloning Kit (Vazyme, China). Plasmids were extracted with a TIANprep Mini Plasmid Kit (TIANGEN Biotech, China). PCR products were recycled and purified using the Universal DNA Purification Kit (TIANGEN Biotech, China).

Genetic Manipulation. The principle of the gene deletion method is illustrated in Figure S2a, and the vectors were constructed based on the plasmid PUC19 (Figure S2b). The gene encoding Ku70 in *M. elegans* strain TTI-0396 was disrupted with a hygromycin B resistance gene to enhance the homologous recombinant frequency. The Ku70 knockout mutant was then used as the recipient strain for biosynthetic gene knockout experiments. Parts of the biosynthetic genes from start codons were replaced by neo markers. The overexpression strains were obtained by insertion of the gpdA promoter in front of the start codon of the target gene.

Knockdown and overexpression of targeted genes were carried out by PEG-mediated transformation of fungal protoplasts.[32,33] Freshly germinated conidia were harvested on Miracloth (Merck-Calbiochem, Germany) and washed with 0.7 M NaCl, then digested with 20 mg/mL Driselase (Sigma-Aldrich) for 2 h. Enzyme lysis products were filtered through Miracloth and washed with STC buffer. The protoplast concentration was adjusted to 1×10^7 cells/mL with STC buffer. Five micrograms of linearized DNA dissolved in 60 μL TEC buffer was added to 100 μL protoplasts and placed on ice for 20 min. Then, 160 μL of 60% PEG4000 (Sigma-Aldrich) was added to the protoplast and incubated at room temperature for 15 min. The total mixture was mixed with 25 mL of melten T-TOP and spread homogeneously on 5 PDA dishes. After culturing at 28 °C for 16−20 h, 10 mL of screening T-TOP was added to each Petri dish. The Ku70 knockout mutant was selected using hygromycin B (35 μg/mL), and other knockout mutants were selected by G418 (35 μg/mL). The screening results of the antibiotic selection concentration are shown in Figure S3. After incubation at 28 °C for 3−5 days, the transformants were transferred to new PDA plates containing corresponding antibiotics. All transformants were subcultured for 3 generations to obtain stable transformants. All mutants were identified by diagnostic PCR. The primers used are listed in Table S2. The electropherograms of the knockout mutants are shown in Figure S2c.

RESULTS AND DISCUSSION

Isolation and Identification of Texenomycins and Lipohexin in *M. elegans* Strain TTI-0396. To isolate enough compounds for structure elucidation and antifungal activity assay, the scaled-up fermentation of *M. elegans* strain TTI-0396 in wheat solid medium was extracted with ethyl acetate. After evaporation of the solvent, the extract was further fractionated through Sephadex LH-20 column chromatography and purified by the preparative reversed-phase HPLC, yielding 58.8 mg of texenomycins. The structure of texenomycins was identified by analyzing its high-resolution electrospray ionization mass spectroscopy (HRESIMS) data (m/z 2029.2827, $[M + H]^+$), which assigned molecular formula to be $C_{96}H_{170}N_{24}O_{23}$, and by comparison of MS/MS ion fragmentation data (Figure 2a) with those described in the literature.[34] As the data agreed well with the values published, the structure of texenomycins was confirmed, as shown in Figure 1. According to previous literature, two epimers, texenomycins A and B, were coisolated from the *M. lindtneri*.[12] They structurally differ in the stereochemistry at C-2 of the proline unit in the polypeptide chain. As the LC-MS chromatogram (Figure 2a) also showed two single peaks, indicating that texenomycins isolated from *M. elegans* strain TTI-0396 are the mixtures of texenomycins A and B epimers. Two minor peaks (epimerization mixtures at C-2) with the same MS/MS ion fragmentation types corresponding to lipohexin (m/z 765.5117, $[M + H]^+$) were detected (Figure 2b), but the quantities were so scarce that we did not attempt purification.

Antifungal Evaluation of Texenomycins. The antifungal activity of texenomycins was measured in a 2-fold liquid dilution series assays (Figure S4). Texenomycins showed strong activities against two plant pathogens, *C. lagenarium* and *B. cinerea*, with MIC values of 1.6 and 3.2 μg/mL, respectively, while, the positive control hygromycin B showed MIC values of 0.8 μg/mL against the two fungal pathogens (Table 1).

Table 1. MIC Values of Texenomycins against Selected Pathogenic Fungi

pathogenic strain	texenomycins (μg/mL)	hygromycin B (μg/mL)
C. lagenarium	1.6	0.8
B. cinerea	3.2	0.8

Genome Characteristics of *M. elegans* Strain TTI-0396. The *M. elegans* strain TTI-0396 genome was assembled into 50 contigs with a genome size of 54.88 Mb and with a contig N50 length of 3.59 Mb (Figure 3a). Its genome size is slightly larger than the genome size of a sequenced *M. elegans* strain NBRC102301 (NCBI accession: GCA_930272665.1), and these two genomes exhibited a highly colinear relationship (Figure S5).[35] Genomic features of two *M. elegans* strains are

https://doi.org/10.1021/acs.jafc.4c08847
J. Agric. Food Chem. 2025, 73, 226−236

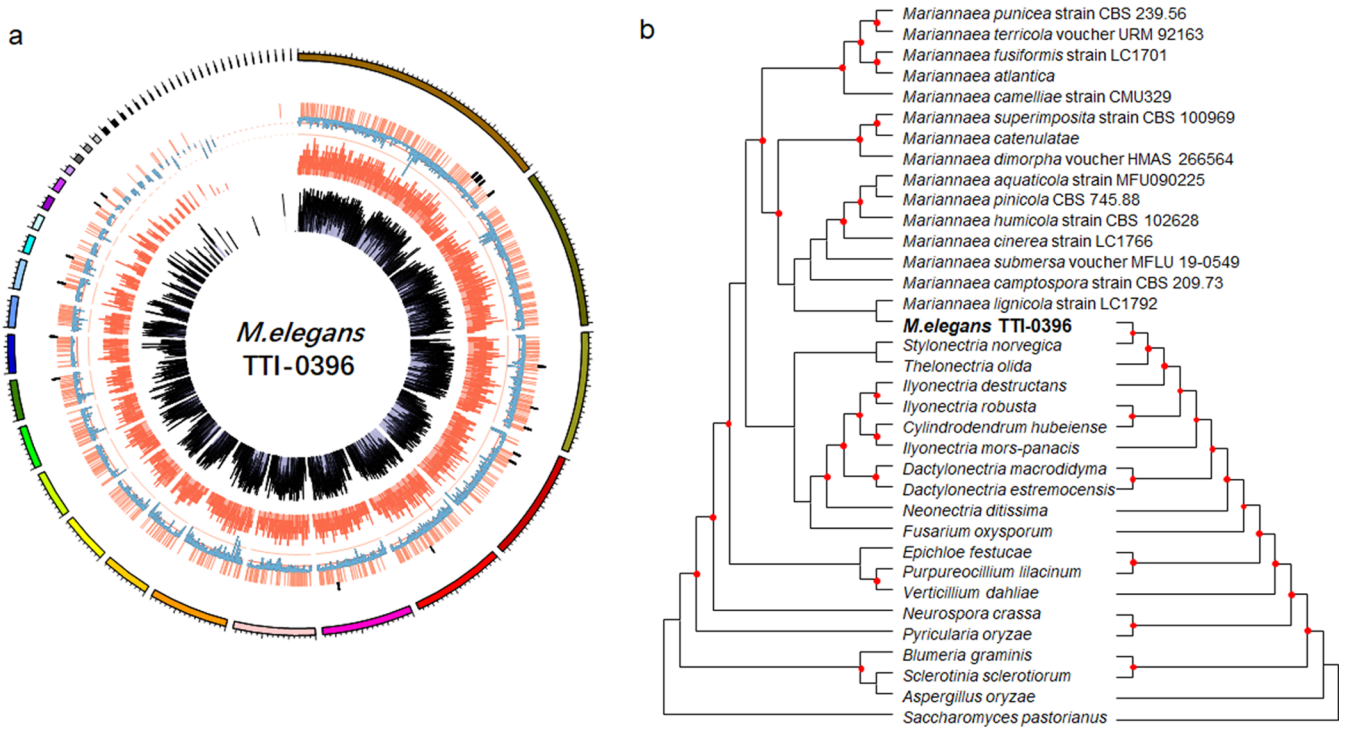

Figure 3. Genome feature and phylogenetic analysis of *M. elegans* strain TTI-0396. (a) Outermost circle is of 50 contigs. Bar chart from outside to inside represents the secondary metabolite gene clusters (black), secreted proteins (orange), density of repetitive sequences (blue), gene density (dark red) and gene expression (FPKM,purple). (b) Evolutionary analysis of *M. elegans* strain TTI-0396 using internal transcribed spacer (ITS) sequence and orthologous genes. Fifteen other species of *Mariannaea*, 10 other species of the family Nectriaceae, 8 species filamentous fungi from other families were chosen to analyze the evolutionary status of *M. elegans* strain TTI-0396. Saccharomyces pastorianus was used as the outgroup. The left-hand tree was constructed from ITS sequences using maximum likelihood method. The right-hand tree was constructed from the concatenated amino acid sequences of common orthologous genes. Branch nodes with greater than 60% support from 1000 bootstrapped pseudoreplicates are indicated with red dots in both trees.

Table 2. Description of Genes in the Texenomycins Biosynthesis Gene Cluster

gene ID	name	length	conserved domain	inferred function
11922	*texA*	189		transcriptional regulator
11923	*texB*	893	LTA_synthase	lipoteichoic acid synthase like
11924	*texC*	279		hypothetical protein
11925	*texD*	714	RING finger-SMC_N	chromatin and DNA dynamics
11926	*texE*	577	DUF2434	hypothetical protein
11927	*texF*	422	b-ZIP	transcriptional regulator
11928	*texG*	8685	(A-PCP-C)*7-A-PCP-TD	NRPS
11929	*texH*	693	acolac_lg	acetolactate synthase
11930	*texI*	593	AMP-binding	acetyl-CoA synthetase and ligase
11931	*texJ*	6457	(C-A-PCP)*6-TD	NRPS
11932	*texK*	394	G-Fe_Oxy_2	dioxygenase
11933	*texL*	310	aldolase_II	aldolases
11934	*texM*	330	RTA1	resistance
11935	*texN*	508	PRK12390-GadA	carboxylate deaminase
11936	*texO*	304	thioesterase	thioesterases
11937	*texP*	311	DH_like_SDR_like	oxidoreduct, dehydratase
11938	*texQ*	2415	KS-DH-MET-ER-KR-ACP	PKS
11939	*texR*	477	bZIP	transcription factor
11940	*texS*	487	MFS	secondary transporter
11941	*texT*	1442	MRP_assoc_pro	ATP-binding cassette transporter
11942	*texU*	266	EntF	thioesterase
11943	*texV*	15,000	(PCP-C-A)*13-PCP-C	NRPS

compared in Table S3. The genome was predicted to have 10,726 protein-coding genes, of which 10,432 (97.3%) were supported by RNA-seq data or were functionally annotated. A combined evolutionary analysis of *M. elegans* strain TTI-0396 was conducted using internal transcribed spacer (ITS) sequences. Orthologous genes confirmed that *M. elegans* strain

https://doi.org/10.1021/acs.jafc.4c08847
J. Agric. Food Chem. 2025, 73, 226−236

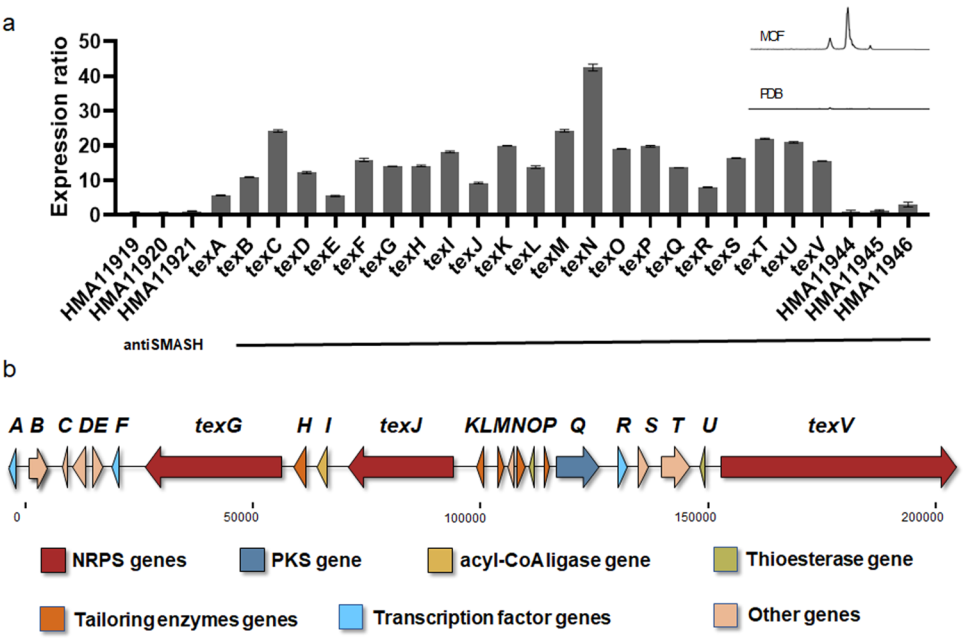

Figure 4. *tex* cluster boundary and organization. (a) Histogram summarizing qRT-PCR analysis and analysis for texenomycins yield by LC-MS. Relative expression is given as a ratio between expression of genes of the WT strain cultured in PDB and MOF media, and the PDB medium was maintained as a control. Error bar indicates the standard deviation (SD). Black straight line indicates the predictions from antiSMASH. The upper right part shows the LC-MS profiles of chemical extracts from the wild-type strain in PDB and MOF cultures. (b) Gene topology of *tex* cluster.

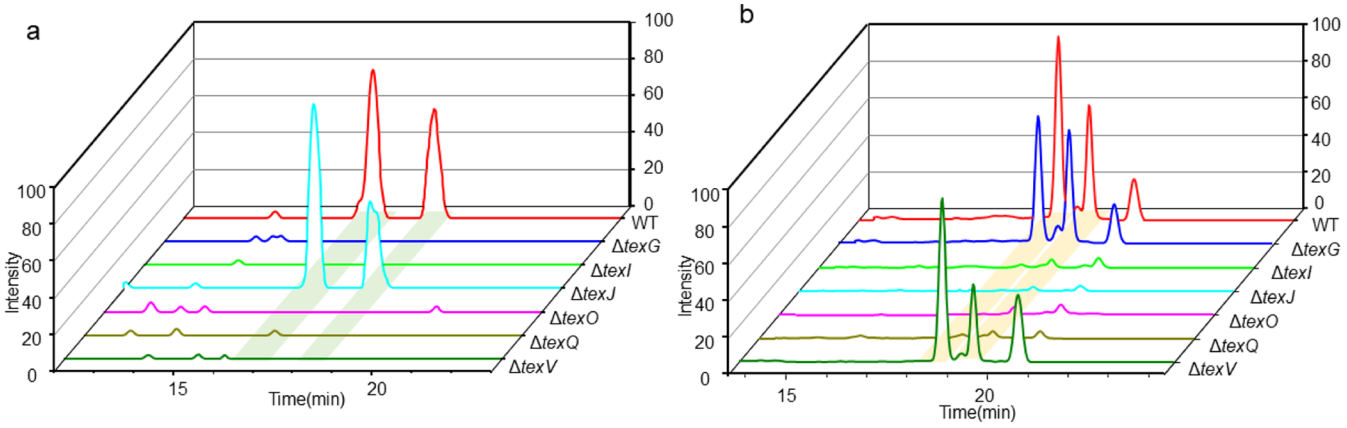

Figure 5. Chemical and analyses of texenomycins and lipohexin produced by the wild-type and mutant strains of *M. elegans* TTI-0396. (a) LC-MS profiles of texenomycins from WT strain and knockout mutants. (b) LC-MS profiles of lipohexin from WT strain and knockout mutants. The peaks observed at 18.6 and 19.4 min correspond to lipohexins, similar to the peak characteristics showed in Figure 2b, while the peak observed at 20.5 min is belong to another compound with identical lipohexin's ionic fragments.

TTI-0396 was congeneric with other fungi in the same genus. *Mariannaea* species were closely related to *Stylonectria norvegica*, *Thelonectria olida*, and *Ilyonectria destructans* in the family Nectriaceae (Figure 3b).

Identification of the Texenomycins Biosynthetic Gene Cluster (*tex*). The secondary metabolites (SMs) of fungi are often species-specific, and we searched the *M. elegans* strain TTI-0396 genome to evaluate its ability to produce SMs. At least 45 SM clusters were identified, including 15 for PKSs, 12 for NRPSs, 4 for PKS-NRPS hybrids, 4 for terpenes, and 1 for indole (Data set S1). Structurally, texenomycins contain a MOTDA fatty acid chain and 21 amino acid residues, suggesting that the *tex* gene cluster likely includes at least PKS and NRPS genes, with the NRPS gene(s) encoding up to 21 modules. Among the identified NRPS and PKS-NRPS hybrid clusters, only one SM cluster contained 21 A domains, and their gene structures and protein domains are illustrated in Figure S6. Based on the prediction of antiSMASH, a PKS-NRPS hybrid gene cluster with 22 genes (from *texA* to *texV*), including one PKS and three NRPS genes, was identified as a candidate (Table 2 and Figure 4). In this cluster, NRPS gene *texG* encodes eight C-A-PCP modules and another NRPS gene *texV* encodes 13 C-A-PCP modules, suggesting that the synthesis of the texenomycins polypeptide chain may result from the collaboration between the two NRPS genes. Furthermore, the PKS gene *texQ*, might be responsible for the biosynthesis of the PKS side chain MOTDA. In addition, two colocalized genes, *texO*, and *texI*, annotated as thioesterase and Acyl-CoA ligase genes, may provide possible mechanisms for the connection of fatty acids and peptides.

Substitutions in the culture media can impact the overall metabolic profile of an organism.[36] In fungi, genes involved in secondary metabolite biosynthesis clusters, such as biosynthetic

https://doi.org/10.1021/acs.jafc.4c08847
J. Agric. Food Chem. 2025, 73, 226−236

and modifying genes, are generally coexpressed. Therefore, the boundaries of the gene cluster can be inferred by detecting the expression levels of related genes in different culture media using qRT-PCR. Texenomycins are typically produced in MOF medium, while it was barely detectable in PDB medium (Figure 4a). The expression patterns of relevant genes when *M. elegans* strain TTI-0396 was grown in two different media (MOF and PDB) were compared by qRT-PCR analysis. Gene expression in the *tex* BGC region from *texA* to *texV* were upregulated at different levels in the MOF medium (Figure 4a). The expression levels for *texG* and *texV* were upregulated by 14-fold and 15-fold, respectively. From these results, we concluded that the 5′ limit of the *tex* gene cluster was *texA*, and the 3′ limit was *texV* (Figure 4b).

Verification of Role of Key Genes in *tex* Cluster for the Biosynthesis of Texenomycins. *Functional Characterization of the PKS, Thioesterase and Acyl-CoA Ligase Genes.* To verify the function of PKS TexQ, the DNA fragment from 300 bp to 2127 bp of *texQ* annotated as KS domain was deleted using a homologous recombination-based method. No texenomycin was detected by LC-MS, indicating that TexQ is involved in the biosynthesis of texenomycins (Figure 5a). In the *tex* gene cluster, there's a thioesterase gene *texO* and an acyl-CoA ligase gene *texI*. Both TexO and TexI showed high identity to the corresponding enzymes of pneumocandin pathway in *Glarea lozoyensis* (98% coverage and 30.8% identity to GLHYD, 95% coverage, and 37.7% identity to GLligase, respectively) and W493 B pathway in *Fusarium pseudograminearum* (96% coverage and 28.4% identity to FPSE_09186, 95% coverage and 31.8% identity to FPSE_09184, respectively), suggesting that they might play similar roles during the synthesis of the PKS side chain of lipopeptide (Figures S7−S10).[37,38] To confirm this hypothesis, these two genes were disrupted in *M. elegans* TTI-0396, respectively. The LC-MS showed that texenomycin was not present in Δ*texI* and Δ*texO* culture, demonstrating the essential function of these genes (Figure 5a). However, we could not detect the polyketide chain MOTDA in these mutants, just like the similar situation we observed in *G. lozoyensis*.[37] Although feeding similar substrates, such as tetradecanoic acid and 2-methyl-hexadecanoic acid, to these mutants, no texenomycins derivatives were produced, suggesting the strict substrate selectivity of NRPS working in the next step.

Functional Characterization of NRPS Genes. The *tex* gene cluster includes three NRPS genes: *texG, texJ*, and *texV*. In order to verify their functions, we disrupted them in *M. elegans* strain TTI-0396, respectively. Based on the LC-MS analysis, texenomycins were produced by *M. elegans* strain TTI-0396 wild-type (WT) and Δ*texJ* strains but were absent in the Δ*texG* and Δ*texV* strains (Figure 5a). This result confirmed that TexG and TexV were essential for the biosynthesis of the texenomycins core structure. To determine the biosynthetic sequence for TexG and TexV, the key residues in the A domain binding pockets of TexG and TexV were predicted by the PKS/NRPS analysis Web site (https://nrps.igs.umaryland.edu/, Table S4). The sequence signatures were almost the same for A1, A4, and A5 in TexG and A2-A5, A8, and A11 in TexV, suggesting the same amino acid selection. Referring to the structure of texenomycins, the positions for A2-A5, A8, A11, A14, and A17−19 were Aib. Furthermore, the thioester reductase domain (TR domain) at the C-terminus of TexG was involved in the release of the product.[39] Therefore, TexV was inferred to be responsible for the synthesis of peptide chains at the N-terminus, while TexG should be responsible for the synthesis of peptide chains at the C-terminus. An evolutionary phylogeny of A domains in the *tex* gene cluster showed that they carrying the same amino acid substrates tended to cluster (Figure S11), supporting the biosynthetic sequence from TexV to TexG.

Verification of Role of Key Genes in *tex* Cluster for the Biosynthesis of Lipohexin. As lipohexin shares the same MOTDA residue at the N-terminus and the first five amino acid residues at the C-terminus with those of texenomycins, and there is only one set of PKS synthetase system (TexQ, TexO, and TexI) and one functionally unknown NRPS (TexJ) encodes six C-A-PCP modules in *tex* gene cluster, which indicated that TexO, TexI, and TexQ might be responsible for the biosynthesis and transfer of MOTDA, and TexJ might be involved in the biosynthesis of the six amino acid residues in lipohexin. To confirm this hypothesis, LC-MS was used to detect the production of lipohexin in Δ*texO*, Δ*texI*, Δ*texQ*, and Δ*texJ* mutants, and no lipohexin peak was observed (Figure 5b). The phylogenetic analysis indicated that A2, A4, A5 in TexJ were grouped with the A domains in TexV and TexG carrying Aib, and A6 in TexJ was grouped with the A domains in TexV and TexG carrying β-Ala, further verifying the TexJ is involved in the synthesis of the peptide chain of lipohexin.

Transcription Factor TexR Upregulated the Production of Texenomycins. Transcriptional regulators within gene clusters are typically essential for controlling the biosynthesis of secondary metabolites. Through gene alignment and functional prediction analysis, TexR, located in *tex* gene cluster, is annotated as a transcription factor. To figure out the function of TexR in texenomycins biosynthesis, gene overexpression or deletion mutants were constructed. Deletion mutants were obtained by replacing the whole gene with a G418 resistance cassette. Overexpression mutants were obtained by replacing the native promoter with the strong constitutive promoter *PgpdA* of *Aspergillus nidulans* (Figure S12), which is widely used to drive the expression of target genes.[40] The yield of texenomycins was analyzed by LC-MS (Figure S13b). The Δ*texR* mutant lost the ability to produce texenomycins, while the yield of texenomycins in the OE*texR* mutant was significantly improved (4-fold). This result indicated that TexR crucially affected the production of texenomycins. Thus, we detected the transcription of the *tex* gene cluster in Δ*texR*, OE*texR* and WT strains by qRT-PCR (Figure S13a). The transcription of all genes in the *tex* cluster decreased due to the deletion of *texR*. Some of the gene expression levels were reduced to one-hundredth of that in WT, including *texD, texK, texM, texN, texP, texQ, and texV*. In OE*texR* mutants, except for *texB, texE, texF, and texH*, the transcription of other genes was upregulated to varying degrees. The expression of *texR* was 161-fold higher in the OE*texR* mutant. Four genes were upregulated by more than 10-fold: *texI* (98-fold), *texL* (66-fold), *texQ* (79-fold) and *texU* (55-fold). Therefore, TexR upregulated the production of texenomycins by regulating the key genes involved in the biosynthesis of texenomycins.

Putative Biosynthetic Pathway for Texenomycins and Lipohexin. By analyzing the gene deletion mutants and RNA expression of the *tex* gene cluster, combined with the LC-MS analysis of gene deletion mutants, we propose a putative biosynthetic pathway for texenomycins in the *tex* gene cluster. MOTDA is synthesized by iterative catalysis of the single-module fungal PKS TexQ and hydrolyzed off the ACP of TexQ by thioesterase TexO. Then, TexI activates and transfers the fatty acid to the first thiolation domain of NRPS TexV or TexJ

https://doi.org/10.1021/acs.jafc.4c08847
J. Agric. Food Chem. 2025, 73, 226−236

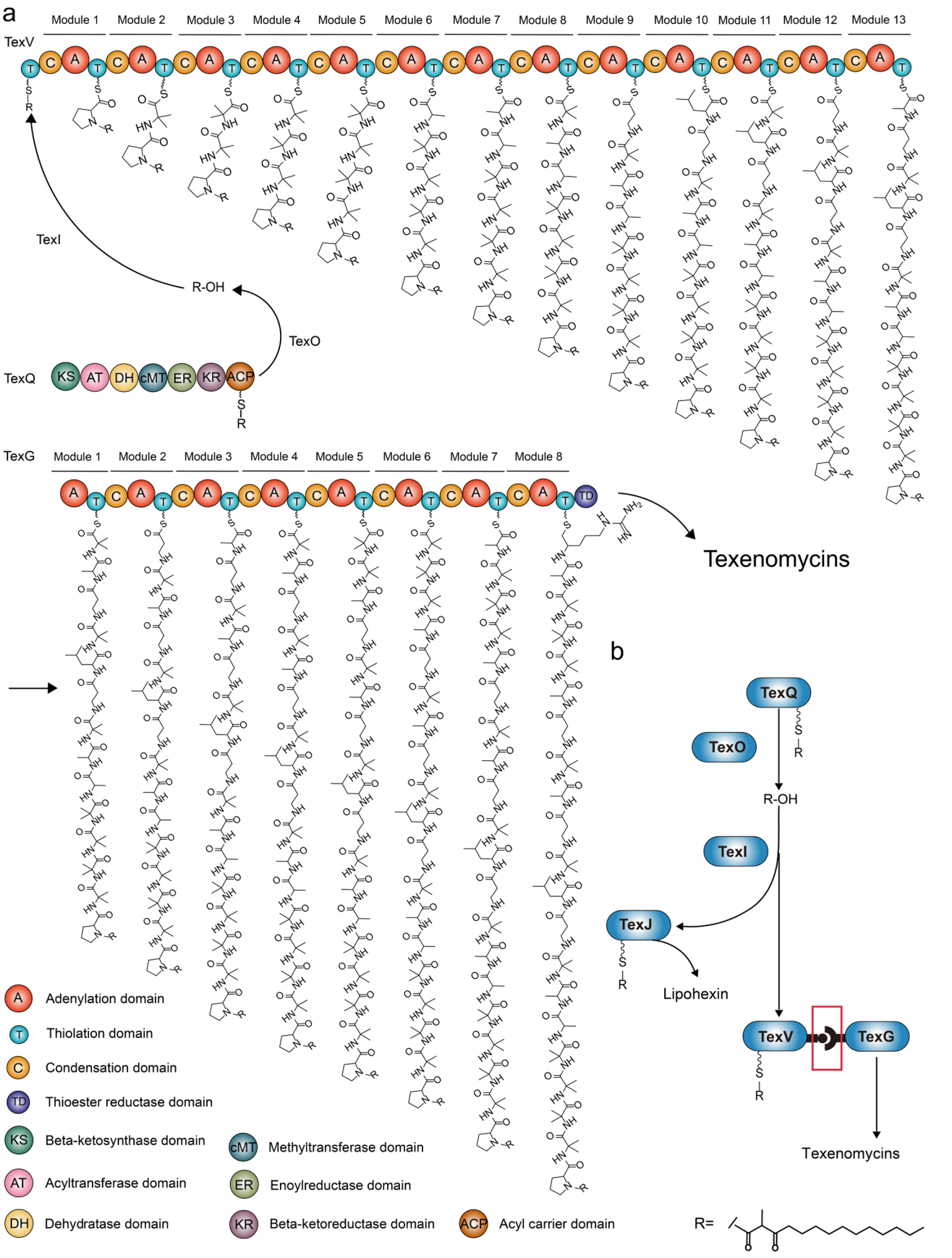

Figure 6. Putative biosynthetic pathway for texenomycins and lipohexin. (a) Putative biosynthetic pathway for texenomycins. (b) The biosynthesis model of texenomycins and lipohexin in *tex* cluster. The red box represents a possible COM domain between TexV and TexG.

https://doi.org/10.1021/acs.jafc.4c08847
J. Agric. Food Chem. 2025, 73, 226−236

(Figure 6a). The backbone of texenomycins is biosynthesized by the cooperation of two NRPSs (TexG and TexV) and the domain localized at the N-terminus of TexG and C-terminus of TexV may function as the communication-mediating (COM) domains like the communication between partner NRPSs in *Bacillus brevis*.[41,42] Although a survey of secondary metabolism gene clusters in fungi suggests that clusters containing more than one NRPS occur, to date, little is known about the crosstalk between colocalized NRPSs in fungi. Lipohexin is proposed synthesized by the PKS system (TexQ, TexO, and TexI) and NRPS (TexJ) (Figure 6b).

The *M. elegans* strain TTI-0396 used in this study was isolated from cow manure, but its role as a coprophilous fungus is uncertain. Based on the known biology of *Mariannaea* species, the fungus might have transiently existed in the manure as a parasite of invertebrates and other fungi. Herbivore dung is a locally rich nutrient-rich and ephemeral ecosystems, encompassing not only a succession of decomposers but also parasites of fungi, insects, and nematodes. This hypothesis is consistent with the previous observation that mycoparasitic and invertebrate parasitic species of the Hypocreales have a strong propensity to produce peptaibols and lipopeptaibols, which contributes to their capacity to invade, kill, and colonize their hosts.[43−45] The coprophilous habitat provides substantial potential for the discovery of new antibiotics from fungi because it represents an important habitat where aggressive specialized saprobes and parasitic fungi coexist.[46]

Our comprehensive analysis led to the successful isolation and identification of lipopeptaibols, texenomycins and lipohexin, from the *M. elegans* strain TTI-0396. Texenomycins exhibited remarkable antifungal activity against two important plant pathogens, *C. lagenarium* and *B. cinerea*, with MICs determined to be 1.6 and 3.2 μg/mL, respectively. These values underscore the potent bioactivity of texenomycins, positioning them as promising candidates for further development as antifungal agents in agriculture.

The genome sequencing of *M. elegans* strain TTI-0396 unveiled a treasure trove of biosynthetic pathways, with a particular focus on the *tex* cluster. This cluster includes a hybrid PKS-NRPS system that is crucial for the biosynthesis of texenomycins and lipohexin. Our subsequent gene knockout experiments provided definitive evidence for the functional roles of six key genes within this system, paving the way for a deeper understanding of the molecular mechanisms underlying the biosynthesis of these bioactive compounds. Based on our gene deletion studies and LC-MS analysis, we propose a putative biosynthetic pathway for texenomycins and lipohexin. This hybrid PKS-NRPS system integrates the iterative catalysis of the single-module fungal PKS TexQ, the hydrolytic action of thioesterase TexO, and the transfer functions of Acyl-CoA ligase TexI. The collaboration between the two NRPSs, TexG and TexV, is hypothesized to generate the texenomycins backbone, with TexV initiating the peptide chain synthesis and TexG responsible for the C-terminus assembly. The domain localized at the N-terminus of the NRPS TexG and C-terminus of another NRPS TexV may function as the communication-mediating (COM) domains like the establishment of communication between partner NRPSs in *Bacillus brevis*.[14] Although a survey of secondary metabolism gene clusters in fungi suggests clusters containing more than one NRPS occur, to date, little is known about the crosstalk between colocalized NRPSs in fungi, but a phenomenon that often occurs in bacteria.[47,48] For example, the orfamide A biosynthetic gene cluster in *Pseudomonas protegens* contains three NRPS genes, and biosynthesis of cereulide in *Bacillus anthracis* contains two NRPS genes, and glidonin biosynthetic gene cluster in *Schlegelella brevitalea* included two NRPS genes.[49,50] In this study, the elucidation of this hybrid PKS-NRPS system advances our comprehension of the production and diversity of lipopeptaibol natural products in fungi.

The transcription factor TexR emerged as a pivotal regulatory element in the biosynthesis of texenomycins. Our findings indicate that TexR upregulates the production of texenomycins, suggesting its critical role in the modulation of gene expression within the *tex* cluster. This discovery opens new avenues for research aimed at enhancing the production of texenomycins through targeted genetic manipulation.

In conclusion, this study has not only expanded the knowledge of fungal natural product biosynthesis but also identified key genetic elements that could be harnessed for the development of new antifungal strategies. The proposed biosynthetic pathway and the regulatory mechanisms uncovered in this study provide a solid foundation for future endeavors in optimizing the production of texenomycins and exploring their application potential in the field of agricultural fungicides.

■ ASSOCIATED CONTENT

Data Availability Statement

The genome data of *M. elegans* strain TTI-0396 has been submitted to National Genomics Data Center of Beijing Institute of Genomics (China National Center for Bioinformation) and Chinese Academy of Sciences under Bioproject PRJCA014477.

Supporting Information

The Supporting Information is available free of charge at https://pubs.acs.org/doi/10.1021/acs.jafc.4c08847.

Morphology of *M. elegans* strain TTI-0396 (Figure S1); knockout strategy by homologous recombination and identification of knockout mutants (Figure S2); response of *M. elegans* strain TTI-0396 to two antibiotics at different concentrations (Figure S3); determination of MIC for texenomycins against fungal pathogens (Figure S4); the synthetic relationship between the genomes of *M. elegans* strains NBRC102301 and TTI-0396 (Figure S5); schematic representations of the functional domains in NRPS and PKS-NRPS hybrid proteins (Figure S6); the alignment results of TexO and GLHYD (Figure S7); the alignment results of TexI and GLligase (Figure S8); the alignment results of TexO and FPSE_09186 (Figure S9); the alignment results of TexI and FPSE_0918 (Figure S10); the unrooted evolution phylogenetic tree of NRPS A domain in tex cluster (Figure S11); overexpression of transcription factor genes *texF* and *texR* (Figure S12); chemical and gene expression analyses of WT and *texR* mutants during texenomycins biosynthesis (Figure S13); genome information for the multiprotein species trees (Table S1); primer sequences used in this study (Table S2); genome features of two *M. elegans* strains (Table S3); specificity prediction of A domains in NRPS (Table S4) (PDF)

The putative secondary metabolic related gene clusters in *M. elegans* TTI-0396 (Data set S1) (PDF)

https://doi.org/10.1021/acs.jafc.4c08847
J. Agric. Food Chem. 2025, 73, 226−236

AUTHOR INFORMATION

Corresponding Authors

Gerald F. Bills − *Texas Therapeutic Institute, The Brown Foundation Institute of Molecular Medicine, University of Texas Health Science Center at Houston, Houston, Texas 77030, United States;* orcid.org/0000-0003-2352-8417; Email: billsge@vt.edu

Bingyan Xie − *State Key Laboratory of Vegetable Biobreeding, Institute of Vegetables and Flowers, Chinese Academy of Agricultural Sciences, Beijing 100081, China;* orcid.org/0000-0001-9640-8956; Email: xiebingyan@caas.cn

Yan Li − *State Key Laboratory of Vegetable Biobreeding, Institute of Vegetables and Flowers, Chinese Academy of Agricultural Sciences, Beijing 100081, China;* orcid.org/0000-0002-4841-9543; Email: liyan05@caas.cn

Authors

Yang Jiao − *State Key Laboratory of Vegetable Biobreeding, Institute of Vegetables and Flowers, Chinese Academy of Agricultural Sciences, Beijing 100081, China; School of Resources and Environment, Henan Institute of Science and Technology, Xinxiang 653003 Henan, China*

Jian Ling − *State Key Laboratory of Vegetable Biobreeding, Institute of Vegetables and Flowers, Chinese Academy of Agricultural Sciences, Beijing 100081, China*

Raja Asad Ali Khan − *State Key Laboratory of Vegetable Biobreeding, Institute of Vegetables and Flowers, Chinese Academy of Agricultural Sciences, Beijing 100081, China;* orcid.org/0000-0001-5767-3466

Ning Luo − *State Key Laboratory of Vegetable Biobreeding, Institute of Vegetables and Flowers, Chinese Academy of Agricultural Sciences, Beijing 100081, China; College of Plant Protection, Gansu Agricultural University, Lanzhou 730070 Gansu, China*

Zixin Li − *State Key Laboratory of Vegetable Biobreeding, Institute of Vegetables and Flowers, Chinese Academy of Agricultural Sciences, Beijing 100081, China*

Zeyu Li − *State Key Laboratory of Vegetable Biobreeding, Institute of Vegetables and Flowers, Chinese Academy of Agricultural Sciences, Beijing 100081, China;* orcid.org/0000-0003-3566-5822

Yuhong Yang − *State Key Laboratory of Vegetable Biobreeding, Institute of Vegetables and Flowers, Chinese Academy of Agricultural Sciences, Beijing 100081, China*

Jianlong Zhao − *State Key Laboratory of Vegetable Biobreeding, Institute of Vegetables and Flowers, Chinese Academy of Agricultural Sciences, Beijing 100081, China*

Zhenchuan Mao − *State Key Laboratory of Vegetable Biobreeding, Institute of Vegetables and Flowers, Chinese Academy of Agricultural Sciences, Beijing 100081, China*

Complete contact information is available at: https://pubs.acs.org/10.1021/acs.jafc.4c08847

Author Contributions

⊥Y.J. and J.L. contributed equally to this work.

Notes

The authors declare no competing financial interest.

ACKNOWLEDGMENTS

This biosynthesis work was supported by grants from the National Key R&D Program of China (2022YFD1400700), the National Natural Science Foundation of China (32272630), and the discovery phase was initiated with support from the National Institutes of Health (R01GM121458). We are also grateful to Wenzhao Wang from Institute of Microbiology Chinese Academy of Sciences for assistance with the LC-MS analysis.

REFERENCES

(1) Savary, S.; Ficke, A.; Aubertot, J. N.; Hollier, C. Crop losses due to diseases and their implications for global food production losses and food security. *Food Secur.* **2012**, *4*, 519−537.

(2) Chen, T.; Zhang, Z.; Chen, Y.; Li, B.; Tian, S. Botrytis cinerea. *Curr. Biol.* **2023**, *33* (11), R460−R462.

(3) Lombard, L.; van der Merwe, N. A.; Groenewald, J. Z.; Crous, P. W. Generic concepts in Nectriaceae. *Stud. Mycol.* **2015**, *80*, 189−245.

(4) Pereira-Dias, L.; Oliveira-Pinto, P. R.; Fernandes, J. O.; Regalado, L.; Mendes, R.; Teixeira, C.; Mariz-Ponte, N.; Gomes, P.; Santos, C. Peptaibiotics: Harnessing the potential of microbial secondary metabolites for mitigation of plant pathogens. *Biotechnol. Adv.* **2023**, *68*, No. 108223.

(5) Gavryushina, I. A.; Georgieva, M. L.; Kuvarina, A. E.; Sadykova, V. S. Peptaibols as potential antifungal and anticancer antibiotics: current and foreseeable development (Review). *Appl. Biochem. Microbiol.* **2021**, *57*, 556−563.

(6) Balázs, D.; Marik, T.; Szekeres, A.; Vágvölgyi, C.; Kredics, L.; Tyagi, C. Structure-activity correlations for peptaibols obtained from clade Longibrachiatum of *Trichoderma*: A combined experimental and computational approach. *Comput. Struct. Biotechnol. J.* **2023**, *21*, 1860−1873.

(7) Marik, T.; Tyagi, C.; Racić, G.; Rakk, D.; Szekeres, A.; Vágvölgyi, C.; Kredics, L. New 19-residue peptaibols from *Trichoderma* Clade Viride. *Microorganisms* **2018**, *6* (3), No. 85.

(8) Alfaro-Vargas, P.; Bastos-Salas, A.; Muñoz-Arrieta, R.; Pereira-Reyes, R.; Redondo-Solano, M.; Fernández, J.; Mora-Villalobos, A.; López-Gómez, J. P. Peptaibol production and characterization from *Trichoderma asperellum* and their action as biofungicide. *J. Fungi* **2022**, *8* (10), No. 1037.

(9) Bolzonello, A.; Morbiato, L.; Tundo, S.; Sella, L.; Baccelli, I.; Echeverrigaray, S.; Musetti, R.; De Zotti, M.; Favaron, F. Peptide Analogs of a Trichoderma Peptaibol Effectively Control Downy Mildew in the Vineyard. *Plant Dis.* **2023**, *107* (9), 2643−2652.

(10) Khare, E.; Kumar, S.; Kim, K. Role of peptaibols and lytic enzymes of *Trichoderma cerinum* Gur1 in biocontrol of *Fusraium oxysporum* and chickpea wilt. *Environ. Sustainability* **2018**, *1*, 39−47.

(11) Sella, L.; Govind, R.; Caracciolo, R.; Quarantin, A.; Vu, V. V.; Tundo, S.; Nguyen, H. M.; Favaron, F.; Musetti, R.; De Zotti, M. Transcriptomic and ultrastructural analyses of *Pyricularia oryzae* treated with fungicidal peptaibol analogs of *Trichoderma* Trichogin. *Front. Microbiol.* **2021**, *12*, No. 753202.

(12) Grigoriev, P. A.; Berg, A.; Schlegel, B.; Heinze, S.; Grafe, U. Formation of anion-selective membrane pores by texenomycin A, a basic lipopeptaibol antibiotic. *J. Antibiot.* **2002**, *55* (9), 826−828.

(13) Heinze, S.; Ritzau, M.; Ihn, W.; Hulsmann, H.; Schlegel, B.; Dornberger, K.; Fleck, W. F.; Zerlin, M.; Christner, C.; Gräfe, U.; Küllertz, G.; Fischer, G. Lipohexin, a new inhibitor of prolyl endopeptidase from *Moeszia lindtneri* (HKI-0054) and *Paecilomyces* sp. (HKI-0055; HKI-0096). I. Screening, isolation and structure elucidation. *J. Antibiot.* **1997**, *50* (3), 379−383.

(14) Fernando, K.; Reddy, P.; Guthridge, K. M.; Spangenberg, G. C.; Rochfort, S. J. A metabolomic study of *Epichloe* endophytes for screening antifungal metabolites. *Metabolites* **2022**, *12* (1), No. 37.

(15) Koren, S.; Walenz, B. P.; Berlin, K.; Miller, J. R.; Bergman, N. H.; Phillippy, A. M. Canu: scalable and accurate long-read assembly via adaptive k-mer weighting and repeat separation. *Genome Res.* **2017**, *27* (5), 722−736.

(16) Jurka, J.; Kapitonov, V. V.; Pavlicek, A.; Klonowski, P.; Kohany, O.; Walichiewicz, J. Repbase Update, a database of eukaryotic repetitive elements. *Cytogenet. Genome Res.* **2005**, *110* (1−4), 462−467.

(17) Burge, C.; Karlin, S. Prediction of complete gene structures in human genomic DNA. *J. Mol. Biol.* **1997**, *268* (1), 78−94.

(18) Korf, I. Gene finding in novel genomes. *BMC Bioinf.* **2004**, *5*, No. 59.
(19) Majoros, W. H.; Pertea, M.; Salzberg, S. L. TigrScan and GlimmerHMM: two open source ab initio eukaryotic gene-finders. *Bioinformatics* **2004**, *20* (16), 2878−2879.
(20) Stanke, M.; Waack, S. Gene prediction with a hidden Markov model and a new intron submodel. *Bioinformatics* **2003**, *19*, ii215−ii225.
(21) Ashburner, M.; Ball, C. A.; Blake, J. A.; Botstein, D.; Butler, H.; Cherry, J. M.; Davis, A. P.; Dolinski, K.; Dwight, S. S.; Eppig, J. T.; Harris, M. A.; Hill, D. P.; Issel-Tarver, L.; Kasarskis, A.; Lewis, S.; Matese, J. C.; Richardson, J. E.; Ringwald, M.; Rubin, G. M.; Sherlock, G. Gene ontology: tool for the unification of biology. The Gene Ontology Consortium. *Nat. Genet.* **2000**, *25* (1), 25−29.
(22) Bairoch, A.; Apweiler, R. The SWISS-PROT protein sequence database and its supplement TrEMBL in 2000. *Nucleic Acids Res.* **2000**, *28* (1), 45−48.
(23) Finn, R. D.; Coggill, P.; Eberhardt, R. Y.; Eddy, S. R.; Mistry, J.; Mitchell, A. L.; Potter, S. C.; Punta, M.; Qureshi, M.; Sangrador-Vegas, A.; Salazar, G. A.; Tate, J.; Bateman, A. The Pfam protein families database: towards a more sustainable future. *Nucleic Acids Res.* **2016**, *44* (D1), D279−285.
(24) Kanehisa, M.; Goto, S.; Kawashima, S.; Okuno, Y.; Hattori, M. The KEGG resource for deciphering the genome. *Nucleic Acids Res.* **2004**, *32*, D277−D280.
(25) Tatusov, R. L.; Fedorova, N. D.; Jackson, J. D.; Jacobs, A. R.; Kiryutin, B.; Koonin, E. V.; Krylov, D. M.; Mazumder, R.; Mekhedov, S. L.; Nikolskaya, A. N.; Rao, B. S.; Smirnov, S.; Sverdlov, A. V.; Vasudevan, S.; Wolf, Y. I.; Yin, J. J.; Natale, D. A. The COG database: an updated version includes eukaryotes. *BMC Bioinf.* **2003**, *4*, No. 41.
(26) Petersen, T. N.; Brunak, S.; von Heijne, G.; Nielsen, H. SignalP 4.0: discriminating signal peptides from transmembrane regions. *Nat. Methods* **2011**, *8* (10), 785−786.
(27) Krzywinski, M.; Schein, J.; Birol, I.; Connors, J.; Gascoyne, R.; Horsman, D.; Jones, S. J.; Marra, M. A. Circos: an information aesthetic for comparative genomics. *Genome Res.* **2009**, *19* (9), 1639−1645.
(28) Emms, D. M.; Kelly, S. OrthoFinder: solving fundamental biases in whole genome comparisons dramatically improves orthogroup inference accuracy. *Genome Biol.* **2015**, *16* (1), No. 157.
(29) Katoh, K.; Standley, D. M. MAFFT multiple sequence alignment software version 7: improvements in performance and usability. *Mol. Biol. Evol.* **2013**, *30* (4), 772−780.
(30) Nguyen, L. T.; Schmidt, H. A.; von Haeseler, A.; Minh, B. Q. IQ-TREE: a fast and effective stochastic algorithm for estimating maximum-likelihood phylogenies. *Mol. Biol. Evol.* **2015**, *32* (1), 268−274.
(31) Livak, K. J.; Schmittgen, T. D. Analysis of relative gene expression data using real-time quantitative PCR and the 2(-Delta Delta C(T)) *Method*. *Methods* **2001**, *25* (4), 402−408.
(32) Bok, J. W.; Keller, N. P. LaeA, a regulator of secondary metabolism in *Aspergillus* spp. *Eukaryotic Cell* **2004**, *3* (2), 527−535.
(33) Li, G.; Li, R.; Liu, Q.; Wang, Q.; Chen, M.; Li, B. A highly efficient polyethylene glycol-mediated transformation method for mushrooms. *FEMS Microbiol. Lett.* **2006**, *256* (2), 203−208.
(34) Grigoriev, P. A.; Schlegel, B.; Kronen, M.; Berg, A.; Hartl, A.; Grafe, U. Differences in membrane pore formation by peptaibols. *J. Pept. Sci.* **2003**, *9* (11−12), 763−768.
(35) Vogt, E.; Field, C. M.; Sonderegger, L.; Künzler, M. Genome sequences of *Rhizopogon roseolus*, *Mariannaea elegans*, *Myrothecium verrucaria*, and *Sphaerostilbella broomeana* and the identification of biosynthetic gene clusters for fungal peptide natural products. *G3: Genes, Genomes, Genet.* **2022**, *12* (7), No. jkac095.
(36) Bode, H. B.; Bethe, B.; Hofs, R.; Zeeck, A. Big effects from small changes: possible ways to explore nature's chemical diversity. *ChemBioChem* **2002**, *3* (7), 619−627.
(37) Chen, L.; Li, Y.; Yue, Q.; Loksztejn, A.; Yokoyama, K.; Felix, E. A.; Liu, X.; Zhang, N.; An, Z.; Bills, G. F. Engineering of new pneumocandin side-chain analogues from *Glarea lozoyensis* by mutasynthesis and evaluation of their antifungal activity. *ACS Chem. Biol.* **2016**, *11* (10), 2724−2733.
(38) Sørensen, J. L.; Sondergaard, T. E.; Covarelli, L.; Fuertes, P. R.; Hansen, F. T.; Frandsen, R. J.; Saei, W.; Lukassen, M. B.; Wimmer, R.; Nielsen, K. F.; Gardiner, D. M.; Giese, H. Identification of the biosynthetic gene clusters for the lipopeptides fusaristatin A and W493 B in *Fusarium graminearum* and *F. pseudograminearum*. *J. Nat. Prod.* **2014**, *77* (12), 2619−2625.
(39) Gacek-Matthews, A.; Chromikova, Z.; Sulyok, M.; Lucking, G.; Barak, I.; Ehling-Schulz, M. Beyond toxin transport: novel role of ABC transporter for enzymatic machinery of cereulide NRPS assembly line. *mBio* **2020**, *11* (5), No. e01577-20.
(40) Liao, X. G.; Fang, W. G.; Zhang, Y. J.; Fan, Y. H.; Wu, X. W.; Zhou, Q.; Pei, Y. Characterization of a highly active promoter, PBbgpd, in *Beauveria bassiana*. *Curr. Microbiol.* **2008**, *57* (2), 121−126.
(41) Ehling-Schulz, M.; Fricker, M.; Grallert, H.; Rieck, P.; Wagner, M.; Scherer, S. Cereulide synthetase gene cluster from emetic *Bacillus cereus*: structure and location on a mega virulence plasmid related to *Bacillus anthracis* toxin plasmid pXO1. *BMC Microbiol.* **2006**, *6*, No. 20.
(42) Hahn, M.; Stachelhaus, T. Selective interaction between nonribosomal peptide synthetases is facilitated by short communication-mediating domains. *Proc. Natl. Acad. Sci. U.S.A.* **2004**, *101* (44), 15585−15590.
(43) Degenkolb, T.; Berg, A.; Gams, W.; Schlegel, B.; Grafe, U. The occurrence of peptaibols and structurally related peptaibiotics in fungi and their mass spectrometric identification via diagnostic fragment ions. *J. Pept. Sci.* **2003**, *9* (11−12), 666−678.
(44) Degenkolb, T.; Kirschbaum, J.; Bruckner, H. New sequences, constituents, and producers of peptaibiotics: an updated review. *Chem. Biodiversity* **2007**, *4* (6), 1052−1067.
(45) Röhrich, C. R.; Jaklitsch, W. M.; Voglmayr, H.; Iversen, A.; Vilcinskas, A.; Nielsen, K. F.; Thrane, U.; von Döhren, H.; Brückner, H.; Degenkolb, T. Front line defenders of the ecological niche! Screening the structural diversity of peptaibiotics from saprotrophic and fungicolous *Trichoderma*/*Hypocrea* species. *Fungal Diversity* **2014**, *69* (1), 117−146.
(46) Bills, G. F.; Gloer, J. B.; An, Z. Coprophilous fungi: antibiotic discovery and functions in an underexplored arena of microbial defensive mutualism. *Curr. Opin. Microbiol.* **2013**, *16* (5), 549−565.
(47) Mootz, H. D.; Marahiel, M. A. The tyrocidine biosynthesis operon of *Bacillus brevis*: complete nucleotide sequence and biochemical characterization of functional internal adenylation domains. *J. Bacteriol.* **1997**, *179* (21), 6843−6850.
(48) Zerikly, M.; Challis, G. L. Strategies for the discovery of new natural products by genome mining. *ChemBioChem* **2009**, *10* (4), 625−633.
(49) Bando, Y.; Hou, Y.; Seyfarth, L.; Probst, J.; Gotze, S.; Bogacz, M.; Hellmich, U. A.; Stallforth, P.; Mittag, M.; Arndt, H. D. Total synthesis and structure correction of the cyclic lipodepsipeptide orfamide A. *Chem. - Eur. J.* **2022**, *28* (20), No. e202104417.
(50) Chen, H.; Zhong, L.; Zhou, H.; Bai, X.; Sun, T.; Wang, X.; Zhao, Y.; Ji, X.; Tu, Q.; Zhang, Y.; Bian, X. Biosynthesis and engineering of the nonribosomal peptides with a C-terminal putrescine. *Nat. Commun.* **2023**, *14* (1), No. 6619.

https://doi.org/10.1021/acs.jafc.4c08847
J. Agric. Food Chem. 2025, 73, 226−236